



ISSN: 0067-2904

Recent Development-1 of CADTEL Software: The Resolution and Focusing Parameters Affecting at the Properties of Electron Magnetic Lenses

Hussain S. Hasan¹, Sura Allawi Obaid², Muhssen Salbookh Erhayief³

^{1,2}Department of Physiology and Medical Physics, College of Medicine, Al-Nahrain University, Baghdad, Iraq

³Department of Physics, College of Education, Mustansiriyah University, Baghdad, Iraq.

Received: 9/12/2020

Accepted: 10/4/2021

Abstract

Computer Aided Designing Tools of Electron Lenses (CADTEL) is a software packages cares about design, compute and plot simultaneously of the objective and projector properties of electron magnetic lenses. The developments in CADTEL software leads to contain a large fields and methods, adding to previous publish in 2013. The current improvement is inserting of some important parameters which are the resolution and focusing parameters. These parameters are angular semi-angle (α), focusing power (β), resolution limit (δ), image rotation (θ), spherical aberration (C_s), defocus (ΔZ), wave aberration (X_{wab}), depth of field (D_{fld}), and depth of focus (D_{foc}) at certain magnification conditions. Thus, user can easily compute and plot, according to relations and forms, the effect of these parameters at the lens properties of four magnification conditions; zero, infinite and finite (low and high) magnification modes. This work introduces a new development for CADTEL software which is an interactive visual interface in electromagnetic lenses. Whereas, it reflects a substantial reduction of time and resources desired for training new users and researchers in electron optics field. The results and curves representations appear with visual interfaces which are coded in visual basic programming language. In addition, the computations and figures which were plotted appeared that complete identification between these results which are obtained from CADTEL and that from other software's and direct computations methods.

Keywords: Magnetic lens, spherical aberration, resolution limit, focusing parameters.

التطوير الحديث-1 لبرنامج CADTEL: معلمات التحليل والتبئير المؤثرة على خواص العدسات الكهرومغناطيسية

حسين صالح حسن¹، سري علاوي عبيد²، محسن صلبوخ ارهيف³

¹، فرع علم وظائف الاعضاء (الفسلجة)، كلية الطب، جامعة النهرين، بغداد، العراق

³ قسم الفيزياء، كلية التربية، الجامعة المستنصرية، بغداد، العراق

الخلاصة

كادتل هو اختصار الاحرف الاولى لجملة أدوات تصميم العدسات الالكترونية بمساعدة الحاسوب. ان تطوير برنامج كادتل تؤدي إلى احتواء مجالات وأساليب كبيرة بالإضافة إلى المنشور سابقاً في عام 2013. التطوير الحالي هو إدخال بعض المعلمات المهمة التي تسمى معلمات التحليل والتبئير. هذه المعلمات هي زاوية الانحراف شبه الزاوي (α)، قوة التبئير (β)، حد التحليل (δ)، دوران الصورة (θ)، الزيغ الكروي (C_s)،

اللاتبئير (ΔZ)، الزئغ الموجي (X_{wab})، عمق المجال (D_{fld})، وعمق التئبئير (D_{foc}) عند شروط تكبئير معينة. وبالتالي يمكن للمستخدم أن يحسب ويرسم بسهولة وفقاً للعلاقات والأشكال، تأثير هذه المعلمات على خصائص العدسة لاربعة شروط تكبئير: النمط الصفري، اللانهائي، النهائي او المحدد (الواطيء والعالي). يهتم هذا العمل بتقديم تطوير جديد لبرنامج CADTEL حيث انه واجهة مرئية تفاعلية في العدسات الكهرومغناطيسية يساعد في تقليص كبير للوقت والموارد المطلوبة لتدريب المستخدمين والباحثين الجدد في مجال البصريات الإلكترونية. تظهر النتائج والمنحنيات مع واجهات مرئية مكتوبة بلغة برمجة فيجوال بيسك. واطهرت نتائج الحسابات والأشكال الحاصلين عليها من كادتل تطابق تام مع النتائج الحاصلين عليها من البرامجيات الأخرى بالإضافة للتطابق مع ما يمكن حسابه بالطرق المباشرة الأخرى.

two types of design procedure. The first one named, analysis procedure (which is based on trial and error) where consist of three sorts called; H1 programs for magnetic scalar potential by solving Laplace's equation [1, 2], H2 and H3 programs for magnetic vector potential by solving Poisson's equation [3, 4] in linear and non linear media respectively. While the second part, named H4 programs for the synthesis procedure (inverse design).

CADTEL software consist of computational and plot steps of magnetic field, equipotential surfaces, flux lines, objective and projector properties, and poles shape for proposed lens design which are appear in auto visual interfaces, that are coded in visual basic language [5].

1. Introduction

CADTEL software was introduced by Hasan in 2013 for electromagnetic lenses. It includes both analysis procedure and synthesis procedure.[1]. Numerous software and simulation programs interested in charged particle optics have been reported such as: G-optk program proposed for object-image analysis mode with intersting capability which was demonstrated by applying this program for three systems of electron optics, the most imported one is a low-energy electron microscopy objective lens [2]; The Electron Optical Design (EOD) software which is a complete workplace for the design of electron and ion microscopes [3]; Charged particle optics (CPO) program which is concerned with imaging and electron physics, optical and electron microscopy, physics of electron devices, particle optics at high and low energies, electron microscopy where the computing methods are used in all these domains [4]; Also there is VDTEL software which is a visual designing tool for electrostatic lenses [5].

2. Case Study

The current paper aims to build and develop a new software CADTEL that can be used to design, compute and plot the resolution and focusing parameters (depending on the objective properties which are determined also in this program) affecting the properties of electron magnetic lenses. The obtained results (computations and figures) are displayed in visual interfaces as a simple way to reduce time and efforts for users and designers in electron optics branch. Thus, the current developed version of CADTEL software, depending upon the synthesis procedure, can be applied to compute and plot the resolution and focusing parameters for 16 mathematical models representing the magnetic flux density of electron magnetic lenses.

Glaser model [6] which takes no.1 in software is the most commonly used as physical (math) model for the flux density of magnetic field generated by a symmetric magnetic lens on the axis. Exponential field model which takes no.3 in software, where it would obviously be beneficial if there was an analytical field distribution that closely resembled the actual field of the lense in order to understand the general behavior of lenses of this kind. Thus, exponential field model can be applied to supply a beneficial initial approximation to focal properties. A lens of this type can also be used as a condenser-objective lens. Other models, such as the bell-shaped model, which is similar to the Gaussian model, which takes no.5 in software, but has a different math function, can be used as well,.Additionally the potential distribution is typically calculated experimentally or numerically. Three-Halfes Exponential model, which

take no.7 in software, is interested in double polpiece lenses. Inverse Tangent Function model, takes no.9 in software and many more.,

The mathematical model of the magnetic field function is used to determine the path of the electron beam as well as determining the distribution of the scalar potential along the supposed optical axis as a starting point in determining the optimal design of the magnetic lens. The benefit of CADTEL and its development is to save time and improve productivity of designers and users with reducing tedious and potential effort [7].

There are three magnification conditions in which an electron lens can be operated. These conditions can be thought of by using any of the two-linearly independent solutions of the paraxial-ray equation. Zero magnification condition required operating state of the charged particle beam enters the electron lens field parallel to the optical axis, i.e. the object position is at infinity. As an example, the final probe-forming lens in a Scanning Electron Microscope (SEM) is usually operated in this condition. While infinite magnification condition, required for the operating condition in this case, is that the image position is at infinity, i.e. the beam emerges from the electron lens field parallel to the optical axis. The objective lens in a Transmission Electron Microscope (TEM) is sometimes operated in this mode. In addition the finite magnification condition requires that the object and the image positions in this operational mode lie at finite distances from the region of the imaging field. The objective lenses in (TEM) are usually operated under this condition. According to the constraints that must be imposed, the finite mode of operation is classified into two types; low magnification condition and high magnification condition [7].

3. Mathematical Representation

The electron lens is a mixture of static or dynamic electrical and magnetic fields, which are used to converge electron streams in a manner similar to an optical lens.

The magnetic field has an affect on the charged beam and deflect it about its path and focuses it in certain point. So, every property or tool that is able to do this , can be called a lens. An electron lens is known as an apparatus that collects and focuses a moving beam of charged particles at the same position.They suffer from very extreme spherical and chromatic aberrations that we normally monitor by inserting small apertures to pick electrons nearest to the optical axis as these are least affected by the aberrations of the lens.

3.1 Abberations

The spherical aberration parameter is one of the objective properties which the integral formula below calculates [8];

$$C_s = \frac{\eta}{128V_r} \int_{z_0}^{z_i} \left[\frac{3\eta}{V_r} B_z^4 r_\alpha^4 + 8B_z^2 r_\alpha^4 - 8B_z^2 r_\alpha^2 r_\alpha'^2 \right] dz \quad (1)$$

Where η is the electron's charge-to-mass quotient. The integration only spans the interval from object plane z_0 to image plane z_i given the limits of the magnetic fields.

Owing to electrons at the edge of the lens, spherical aberration is bent compared to that in the centre because there is no uniform magnetic field between the pole pieces of the lens. Spherical aberration results in unsharp point and distortion of the image, which can be fixed with a small aperture.

The wave aberration function is defined as the difference of phase or distance in the optical path from the perfect spherical wave (reference) to the actual wavefront for the proposed lens. Since the area on the sample that is viewed most of the time in EMs (especially in TEMs) is quite small, it is usually possible to ignore the dependency of the wave aberration function on the position of the point source in the object plane, this is known as the isoplanctic approximation [9].

The wave aberrations (X_{wab}) in the EM images generate a scrambling of amplitude and phase detail. In addition, a minor misalignment of the path of the incident electron beam causes wave aberrations and thus affects the image quality so that coma-free alignment is necessary for HRTEM [9].

The X_{wab} is defined as the sum of spherical aberration (C_s) and defocus (ΔZ) [10]. i.e.;

$$X_{wab} = C_s + \Delta Z \tag{2}$$

$$\Delta Z = (\lambda \cdot C_s)^{1/2} \tag{3}$$

Where λ the electrons wavelength. So, by substituting equation (3) in equation (2) yeild;

$$X_{wab} = C_s [1 + (\lambda / C_s)^{1/2}] \tag{4}$$

Also, the wave aberration can defined as,

$$X_{wab} = \pi \theta^2 (C_s / \lambda)^{1/2} \tag{5}$$

Thus, depending on $X_{wab} = \pi \Delta Z \theta^2 / \lambda$ and $\Delta Z \leq \lambda / \theta^2$, the result that $X_{wab} \leq \pi$ is reached.

3.2 Semi-angle Aperture

Lens apertures was used to monitor the divergence or convergence of electron paths through the lenses that, in effect, influence the aberrations of the lens and regulate the current in the beam that reaches the specimen.

The semi-angle aperture or divergence angle (α) is related with spherical aberration coeffiecint (C_s) by the form [11]:

$$\alpha \text{ (rad)} = (\lambda / C_s)^{1/4} \tag{6}$$

It should be remmebered that the wavelength (λ in nm) is related with the accelerated potential V_r (in volt) of electron beam by the form [7]:

$$\lambda \text{ (nm)} = (h^2 / 2emV_r)^{1/2} = (1.5 / V_r)^{1/2} \tag{7}$$

Thus, the semi-angle (α) takes the form:

$$\alpha \text{ (rad)} = 0.006 / (C_s^{1/4} V_r^{1/8}) \tag{8}$$

So, the optimum angular semi-angle aperture (α) is given by [11]:

$$\alpha_{opt} \text{ (rad)} = (\lambda / C_s)^{1/4} \tag{9}$$

3.3 Focal Length and Focusing Power

The focusing power β is the ability to refract the electron beam toward the optic axis. It is equal to reciprocal of the focal length:

$$\beta = 1/f \quad \text{(in unit m}^{-1}\text{)} \tag{10}$$

According to Rayleigh criterion, the resolution limit (δ) is formed as [11]:

$$\delta = 0.61 (C_s \lambda^3)^{1/4} \tag{11}$$

The value of the constant in the last equation depends on aperture shape and its value equal to 0.61 for circular aperture.

The effect of the magnetic forces acting on a charged particle in the approximation of the thin lens leads to a simple relationship for a magnetic lens' focusing strength [12]:

For electrons :

$$f = 7.245 \times 10^{-5} V_r / (B_{max} NI) \tag{12}$$

$$\beta = 1/f = 13802 B_{max} NI / V_r \tag{13}$$

where B_{max} is the maximum magnetic field density value, μ_0 is the magnetic permeability in vacuum ($4\pi \times 10^{-7} \text{ Hm}^{-1}$), and NI is Ampere-turns number of the magnetizing coil (lens excitation).

The focusing power varies with changing the current (I) provided by the coil windings (N) or excitation of the electron lens, because the maximum value of magnetic field density (B_m) is proportional with this current. This ability to change the focal length f means that an electron image can be converged by changing the current of the lens.

Simple comparison between electrons and other charged particles (for the same I and KE or V_r), it can be seen that the focusing power of the magnetic lens is much smaller for other particles (not electrons) whose mass is thousands of times greater than that of the electron. Ion optics usually includes electrostatic lenses for this purpose.

3.4 Image Rotation

The plane of the exit ray is rotated at angle (θ) with comparison to the plane of the incoming electron. The total angle of rotation for the image along the interval confined between the

object (z_o) and the image (z_i) positions can be found by integrating one of the components of the paraxil ray equation [7]:

$$d\theta/dz = \sqrt{e/8mV_r} B_z \tag{14}$$

to result:

$$\theta = \sqrt{e/8mV_r} \int_{z_o}^{z_i} B_z dz \tag{15}$$

According to Ampere's law

$$\int_{-\infty}^{\infty} B_z dz = \mu_0 NI \tag{16}$$

Equation (15) can be modified to the following expression [7]:

$$\theta = \sqrt{(e \mu_0^2/8m)} (NI/\sqrt{V_r}) = \sqrt{(e \mu_0^2/8m)} [(V_{z_1} - V_{z_2})/\sqrt{V_r}] \tag{17}$$

For electrons specifically, the last equation becomes:

$$\theta \text{ (rad)} = 0.1863 (NI/\sqrt{V_r}) \tag{18}$$

In case of reversing the current passing through the coil windings of the electron lens, the image rotation would reverse, because the axial magnetic flux density B_z (and also θ) would be reversed in sign. Therefore, inverting the current does not vary the focusing power, because its equation contains B_z^2 which is always positive.

3.5 Depth of Focus and Depth Field

The field depth (D_{fld}) is measured at the target and refers to it. It is the distance on either side of the object plane along the axis through which the object can be moved without visible loss of focus in the image.

The focus depth (D_{foc}) is measured in the image plane and refers to it. This is the distance on both sides of the image plane along the axis on which the image is centered and the focal plane and objective lens are fixed, as illustrating in Figure 1 [13].

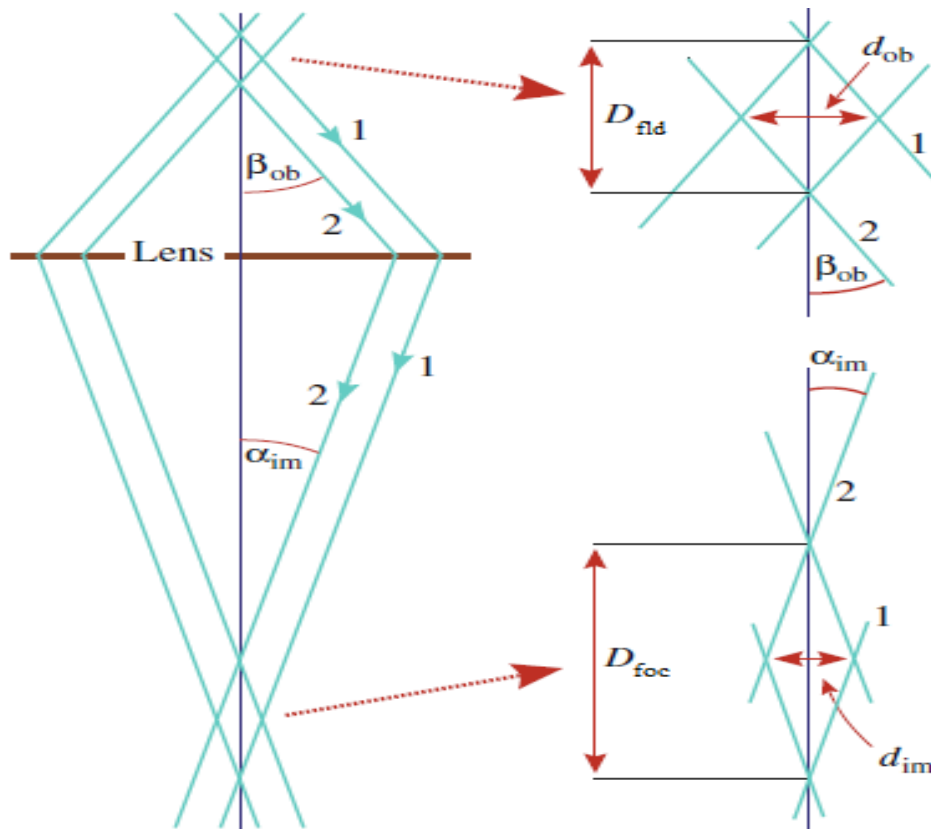


Figure 1- Schematic diagram illustrating the depth of focus and depth of field.

Thus, the ray paths 1 and 2 (Figure 1) remain in focus when emerging $\pm D_{fld}/2$ each side of a plane in the specimen. It can be mentioned that, usually D_{fld} must be greater than the thickness of the specimen. The same rays describe the D_{fld} over which each side of the image plane is in focus $\pm D_{foc}/2$. Where the object's resolution is d_{ob} , and that of the image is d_{im} . So, D_{fld} is equal to:

$$D_{fld} \text{ (nm)} = \delta \text{ (nm)} / \tan \alpha \tag{19}$$

Depth of focus is the ability to converge lineaments within the same image at different depths, or the ability to produce a sharp image from a non-flat surface.

$$D_{foc} \text{ (nm)} = \lambda \text{ (nm)} / n \sin \alpha = \lambda \text{ (nm)} / \sin \alpha \quad \text{when } n=1 \text{ for air} \tag{20}$$

4. Visual Interfaces

The current improved CADTEL software contains a multiple of interfaces, as shown in Figure 2, with a lot of commands that are executed as computations and plots, as illustrated in Figure 3.

5. Data Set

The interfaces and home page automatically give the freedom to choose the required mathematical model and inserting desirable data to obtain the useful flux distribution of magnetic density and scalar magnetic potential, each is plotted as a function of axial distance. In addition, the objective and projection properties are plotted as a function of the accelerating voltage (V_r) and excitation parameters ($NI/\sqrt{V_r}$). CADTEL software can store data in an external file which can be edited by the user in text boxes in the home page. Also, output results can be received with auto display appearing in text boxes and can be saved in external file which is prepared previously.

6. System Modeling

The CADTEL software is an important new tool for designing and analyzing electromagnetic lenses. This software offers an interactive and intuitive programming package in both the analysis and synthesis process for designing symmetric and asymmetric lenses for more than pole-piece under four operating conditions. CADTEL reflects a substantial decrease in the working time and resources desired for educating new users in the use of electron optics programs. Therefore, the since of the field of electron optics should be realizing improved efficiency.

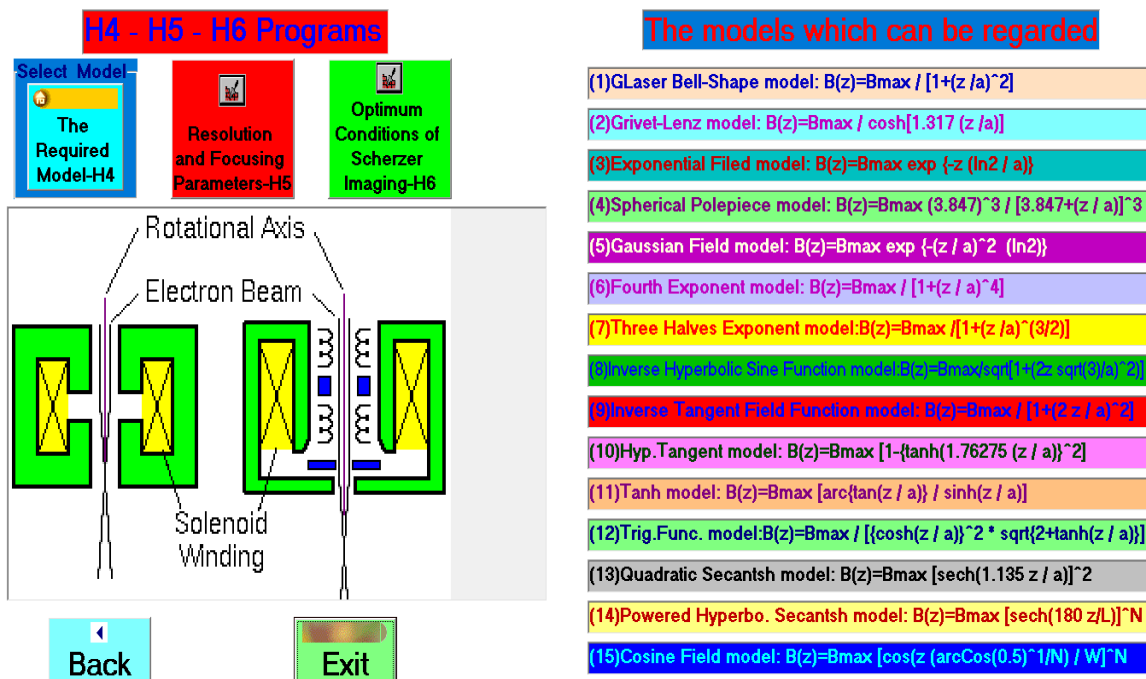


Figure 2- Visual interface pages for the CADTEL software.

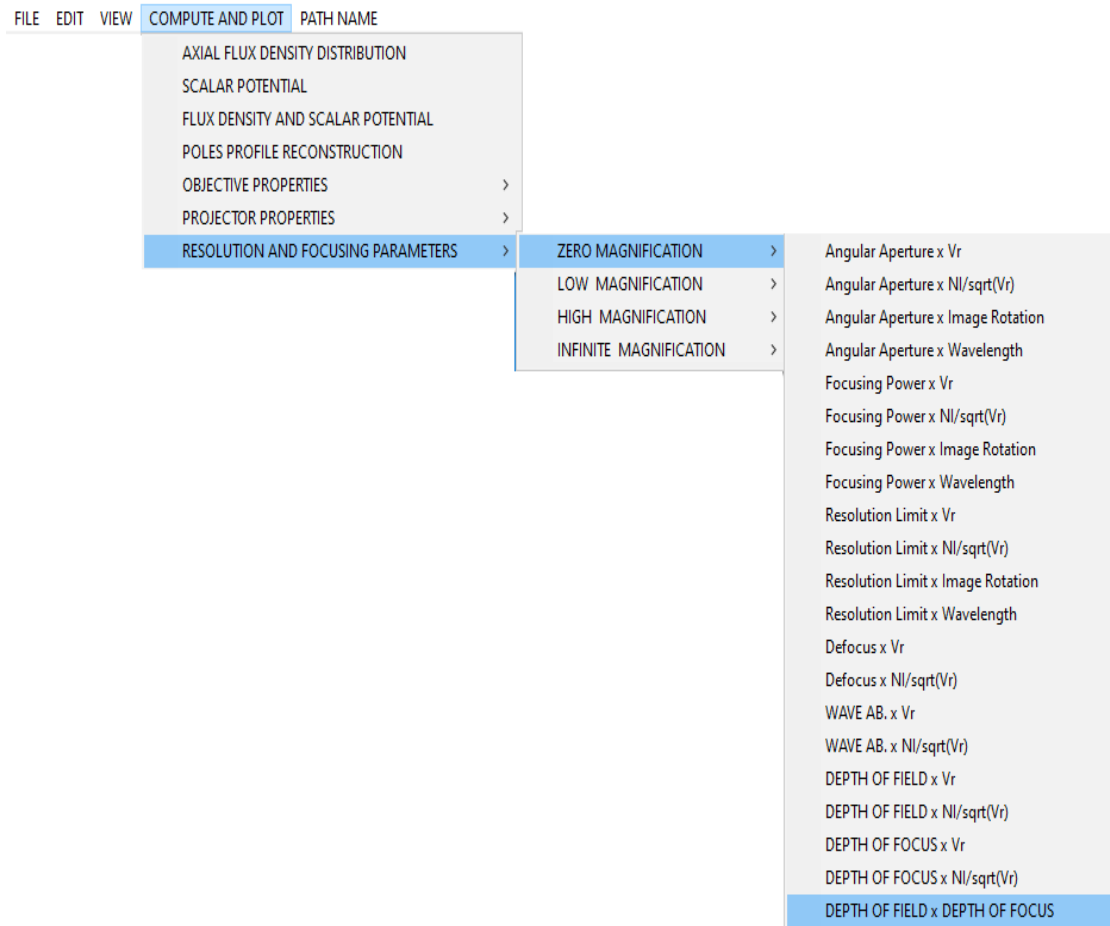


Figure 3- The commands can be executing as computations and plots at developing of CADTEL software.

7. Results and Discussion

The outcome results supply searcher beneficial feedback about the proposed model (lens) from auto use in FILE, EDIT, VIEW, COMPUTE AND PLOT, PATH NAME, and HELP options which are available in a task bar according to user need (see Figure 3).

If model no.=3 is selected, $B_{max}=0.1$ Tesla, $z_1=-10$ mm, $a_1=0.75$ mm, $a_2=0.75$ mm (symmetric lens) for exponential field model and using its magnetic flux density (B_z) and zero magnification condition as a case study to compute the resolution and focusing parameters as in Table 1 and plot these parameters with each other to study its behaviors. Note the user can select any model, magnetic flux density, and other variables, i.e. can be choose multiple lenses for all types of magnification conditions.

Table 1: The resolution and focusing parameters of proposed magnetic lens for zero magnification condition

BEAM VOLTAGE	EXCITATION PARAMETER	WAVE LENGTH	ANGLE IMAGE ROTATION	FOCAL LENGTH	SPHER. AB.	ANGULAR APERTURE	FOCUSING POWER	RESOLUTION LIMIT	DEFOCUSING	WAVE AB.	DEPTH OF FIELD	DEPTH OF FOCUS
V_r (Kv)	$NI/\sqrt{V_r}$ (A)	λ (nm)	θ (rad)	f_o (m)	C_s (m)	α (rad)	β (1/m)	δ (nm)	ΔZ (m)	X_{wab}	D_{fld} (m)	D_{foc} (nm)
29.6628	1	0.00711	0.1863	0.12473	885.59383	0.0003036	8.01748	14.49082	0.00007936	0.0012162	0.00004773	23.42197
7.4157	2	0.01422	0.3726	0.03149	14.36378	0.0010117	31.75727	8.69709	0.00001429	0.0004381	0.0000086	14.05739
3.2959	3	0.02133	0.5589	0.01423	1.34198	0.0020252	70.29276	6.51721	0.00000535	0.000246	0.00000322	10.53397
1.8539	4	0.02844	0.7452	0.00819	0.26052	0.0032785	122.11682	5.36769	0.00000272	0.0001669	0.00000164	8.67598
1.1865	5	0.03556	0.9315	0.0054	0.07629	0.0047124	185.19679	4.66805	0.00000165	0.0001262	0.00000099	7.54514
0.824	6	0.04267	1.1178	0.00389	0.0292	0.0062708	257.06332	4.20957	0.00000112	0.0001026	0.00000067	6.80411
0.6054	7	0.04978	1.3041	0.00299	0.0135	0.0079032	334.99404	3.89678	0.00000082	0.0000879	0.00000049	6.29856
0.4635	8	0.05689	1.4904	0.0024	0.00718	0.0095688	416.31032	3.67827	0.00000064	0.0000784	0.00000038	5.94539
0.3662	9	0.064	1.6767	0.00201	0.00425	0.0112386	498.62892	3.52323	0.00000052	0.0000719	0.00000031	5.69483
0.2966	10	0.07111	1.863	0.00172	0.00273	0.0128905	579.81919	3.41302	0.00000044	0.0000675	0.00000026	5.51673
0.2451	11	0.07822	2.0493	0.00152	0.00186	0.0145194	658.58056	3.33315	0.00000038	0.0000643	0.00000023	5.38766
0.206	12	0.08533	2.2356	0.00136	0.00134	0.0161086	733.27965	3.27741	0.00000034	0.0000622	0.0000002	5.29762
0.1755	13	0.09244	2.4219	0.00125	0.00101	0.0176378	802.32254	3.24271	0.00000031	0.0000609	0.00000018	5.24157
0.1513	14	0.09956	2.6082	0.00115	0.00079	0.019139	866.79284	3.21824	0.00000028	0.00006	0.00000017	5.20206
0.1318	15	0.10667	2.7945	0.00108	0.00063	0.020569	924.66235	3.20839	0.00000026	0.0000596	0.00000016	5.18618
0.1159	16	0.11378	2.9808	0.00103	0.00052	0.0219117	975.32979	3.21257	0.00000024	0.0000598	0.00000015	5.19299
0.1026	17	0.12089	3.1671	0.00098	0.00045	0.0231337	1017.88071	3.23305	0.00000023	0.0000605	0.00000014	5.22615
0.0916	18	0.128	3.3534	0.00094	0.00038	0.0243614	1058.44148	3.25071	0.00000022	0.0000612	0.00000013	5.25475
0.0822	19	0.13511	3.5397	0.00092	0.00035	0.0253664	1087.5969	3.29537	0.00000022	0.0000629	0.00000013	5.32698
0.0742	20	0.14222	3.726	0.0009	0.00032	0.0261301	1105.7607	3.36742	0.00000021	0.0000657	0.00000013	5.44349

THE ABOVE RESULTS ARE FOR AN EXCITATION OF NI = 172.23 AMPURNS

From command task, if the designer choose the state of zero magnification condition, the angular aperture (α) can be computed and plotted as a function of V_r , $NI/\sqrt{V_r}$, θ , and λ , as illustrated in Figures 4, 5, 6, and 7, respectively. From these curves, it can be seen that α reduces with the increment of V_r , while it increases with increasing the values of $NI/\sqrt{V_r}$, θ , and λ . Therefore, the focusing power (β) can be computed and plotted as a function of V_r , $NI/\sqrt{V_r}$, θ , and λ , as shown in Figures 8, 9, 10, and 11, respectively. Which are illustrated from curves path in x-y coordinates of these figures, β is decreasing with the growth of V_r , thus, it increases with the growth of $NI/\sqrt{V_r}$, θ , and λ . Also the resolution limit (δ) can be computed and plotted as a function of V_r , $NI/\sqrt{V_r}$, θ , and λ , as noticed in Figures 12, 13, 14, and 15, respectively. It is clear from the behavior of the curves in these figures that δ increases with increasing V_r , while it reduces with increasing $NI/\sqrt{V_r}$, θ , and λ . Thus, the defocus (ΔZ) can be computed and plotted as a function of V_r , and $NI/\sqrt{V_r}$, as illustrated in Figures 16, and 17, respectively. It can be noticed, from these figures, that ΔZ grows with increasing V_r , but reduces with increasing $NI/\sqrt{V_r}$. In addition, the wave aberration (X_{wab}) can be computed and plotted as a function of V_r , and $NI/\sqrt{V_r}$, as shown in Figures 18, and 19, respectively. From these figures, it is noted that X_{wab} increases with the growth of V_r , while it decreases with increasing $NI/\sqrt{V_r}$. In addition, the depth of field (D_{fld}) can be computed and plotted as a function of V_r , and $NI/\sqrt{V_r}$, as noticed in Figures 20, and 21, respectively. Thus, the user can notice from these figures that D_{fld} grows with increasing V_r , but decay with increasing $NI/\sqrt{V_r}$. The depth of focus (D_{foc}) can be computed and plotted as a function of V_r , and $NI/\sqrt{V_r}$, as illustrated in Figures 22, and 23, respectively. It can be noticed, from these figures, that D_{foc} go up exponentially with the increase of V_r , while it drops exponentially with increasing $NI/\sqrt{V_r}$. Finally, the depth of field (D_{fld}) can be computed and plotted as a function of depth of focus (D_{foc}), as shown in Figure 24. From this figure, the exponentially increase of D_{fld} with increasing D_{foc} can be noted.

From the above figures and behavior of the curves, the designer and user for this software and the currents development, can view the relation of the variations (increments and decrements) depending according to data selected and model or design which is provided.

8. Conclusion

At zero magnification condition (ZMC), increasing the angular aperture and focusing power would be associated with high values of excitation parameter, image rotation, and wavelength, and low values of accelerating voltage. While the resolution limit reaches lower values with increasing each of the excitation parameter, image rotation, and wavelength, and decreasing accelerating voltage.

Thus, the defocus increases with high values of accelerating voltage and low values of excitation parameter. As well, decreasing the wave aberration should be associate with low values of accelerating voltage and high values of excitation parameter.

Therefore, increasing the field depth and focus depth with high values of accelerating voltage and low values of excitation parameter. So, the depth of field will increase with increasing the depth of focus.

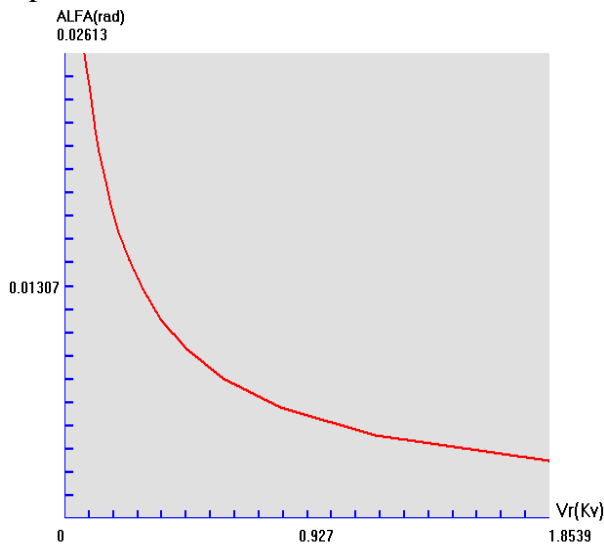


Figure 4- The angular aperture (α) as a function of accelerating voltage (V_r) at ZMC for magnetic lens with using the exponential field model.

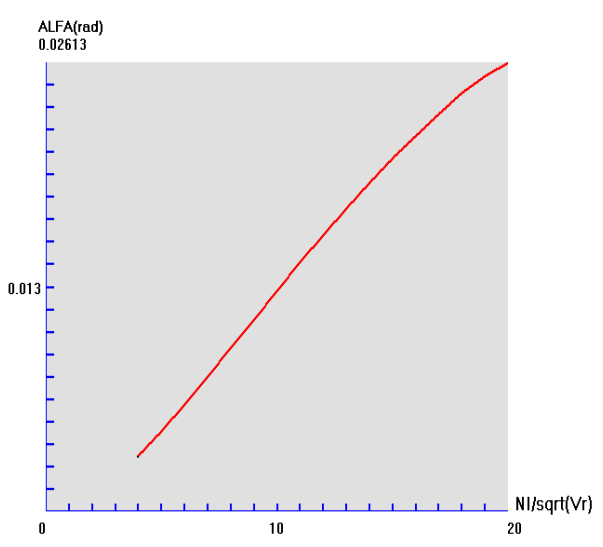


Figure 5- The angular aperture (α) as a function of excitation parameter ($NI/\sqrt{V_r}$) at ZMC for magnetic lens with using the exponential field model.

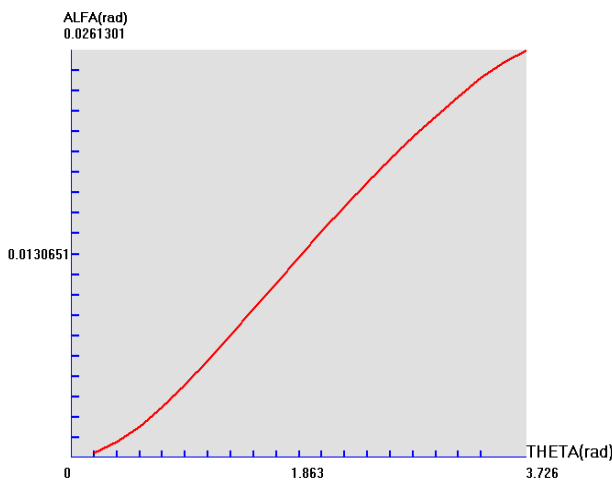


Figure 6- The angular aperture (α) as a function of image rotation (θ) at ZMC for magnetic lens with using the exponential field model.

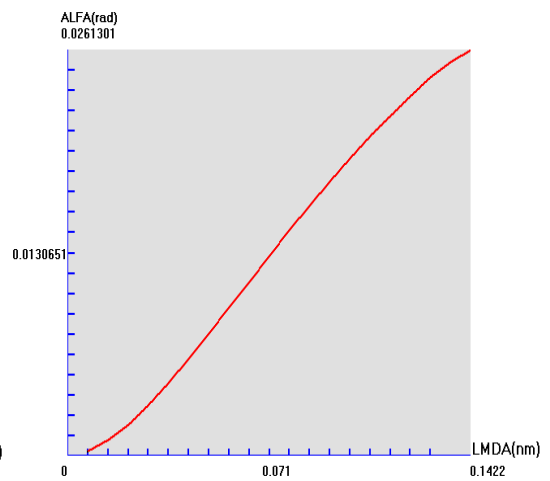


Figure 7- The angular aperture (α) as a function of wavelength (λ) at ZMC for magnetic lens with using the exponential field model.

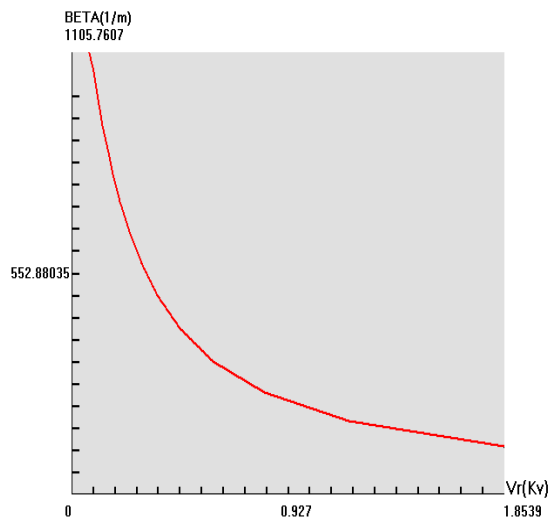


Figure 8- The focusing power (β) as a function of accelerating voltage (V_r) at ZMC for magnetic lens with using the exponential field model.

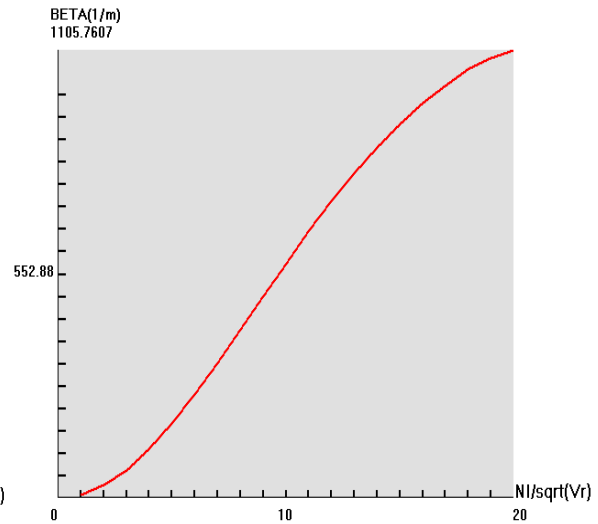


Figure 9- The focusing power (β) as a function of excitation parameter ($NI/\sqrt{V_r}$) at zero magnification condition ZMC for magnetic lens with using the exponential

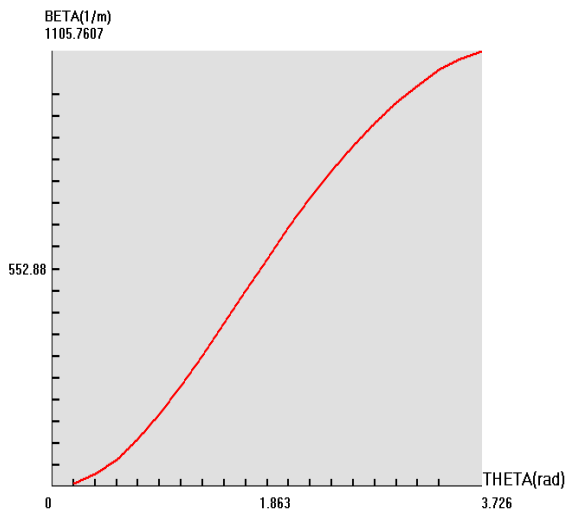


Figure 10- The focusing power (β) as a function of image rotation (θ) at ZMC for magnetic lens with using the exponential field model.

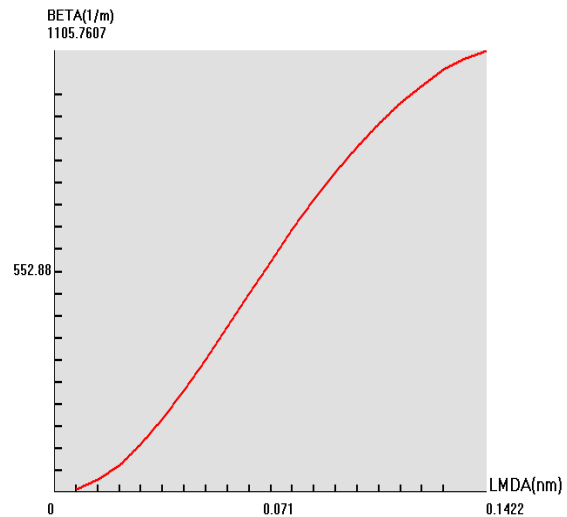


Figure 11- The focusing power (β) as a function of wavelength (λ) at ZMC for magnetic lens with using the exponential field model.

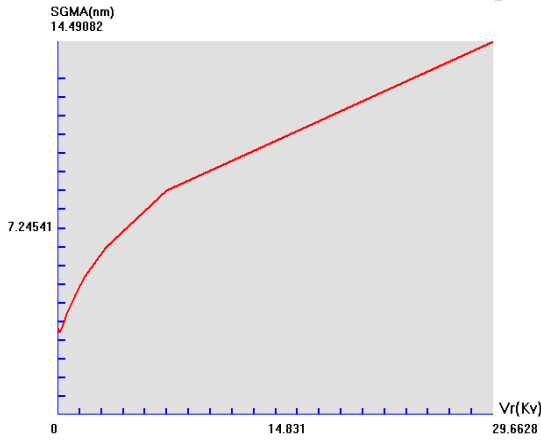


Figure 12- The resolution limit (δ) as a function of accelerating voltage (V_r) at ZMC for magnetic lens with using the exponential field model.

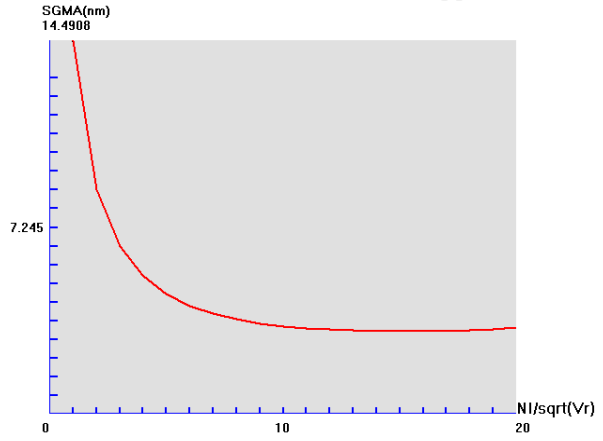


Figure 13- The resolution limit (δ) as a function of excitation parameter ($NI/\sqrt{V_r}$) at ZMC for magnetic lens with using the exponential field model.

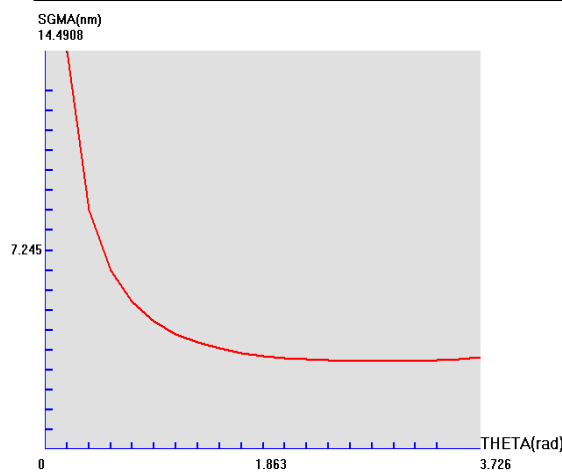


Figure 14- The resolution limit (δ) as a function of image rotation (θ) at ZMC for magnetic lens with using the exponential field model.

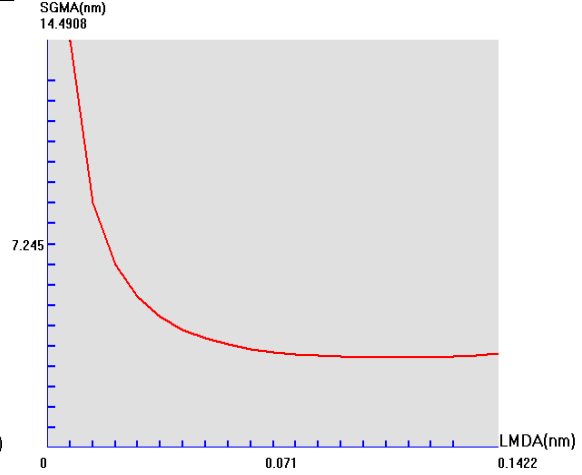


Figure 15- The resolution limit (δ) as a function of wavelength (λ) at ZMC for magnetic lens with using the exponential field model.

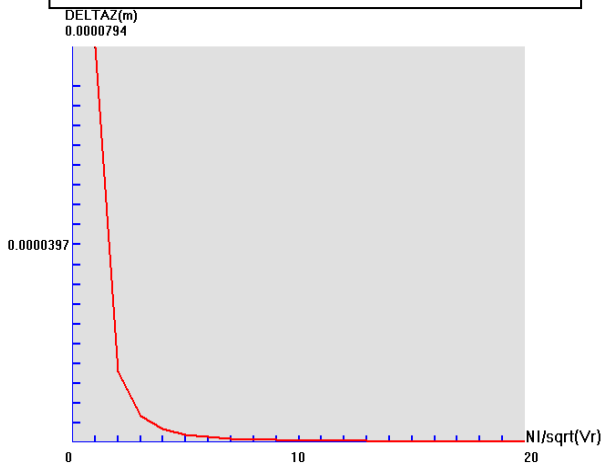


Figure 16- The defocus (ΔZ) as a function of accelerating voltage (V_r) at ZMC for magnetic lens with using the exponential field model.

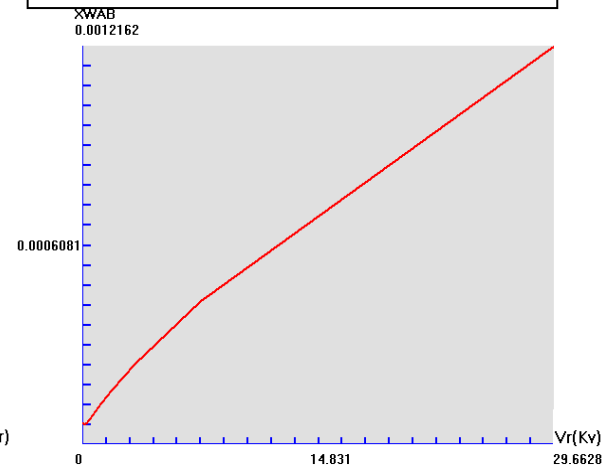


Figure 17- The defocus (ΔZ) as a function of excitation parameter ($NI/\sqrt{V_r}$) at ZMC for magnetic lens with using the exponential field model.

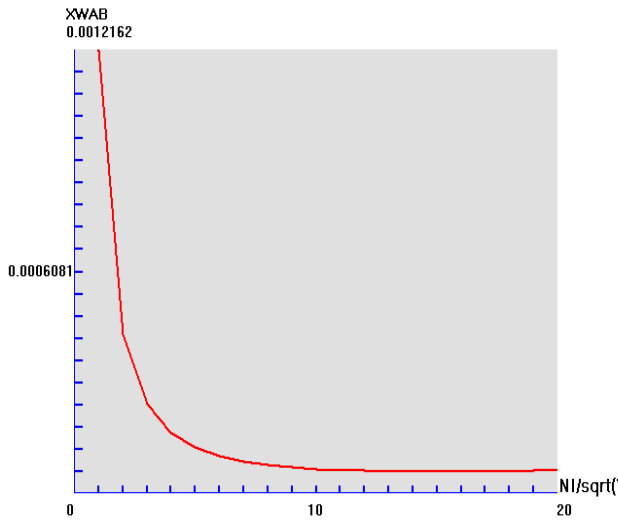


Figure 18- The wave aberration (X_{wab}) as a function of accelerating voltage (V_r) at ZMC for magnetic lens with using the exponential field model.

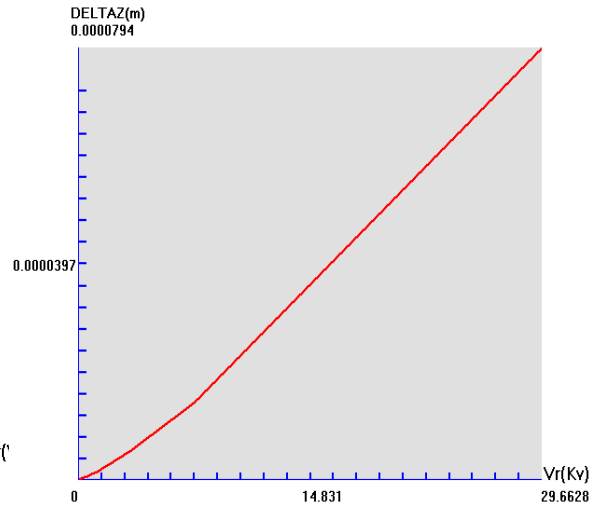


Figure 19- The wave aberration (X_{wab}) as a function of excitation parameter ($NI/\sqrt{V_r}$) at ZMC for magnetic lens with using the exponential field model.

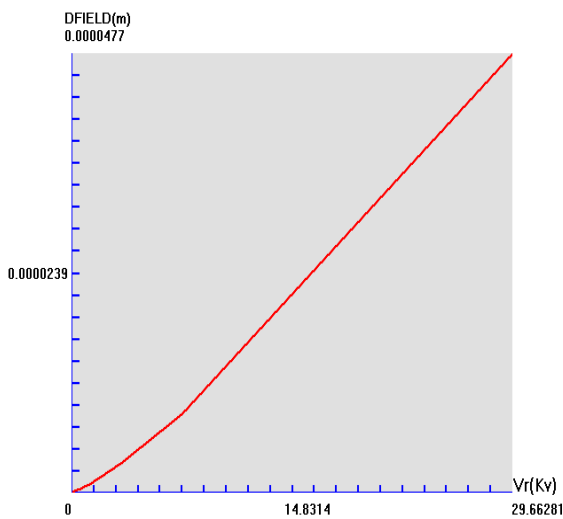


Figure 20- The depth of field (D_{fld}) as a function of accelerating voltage (V_r) at ZMC for magnetic lens with using the exponential field model.

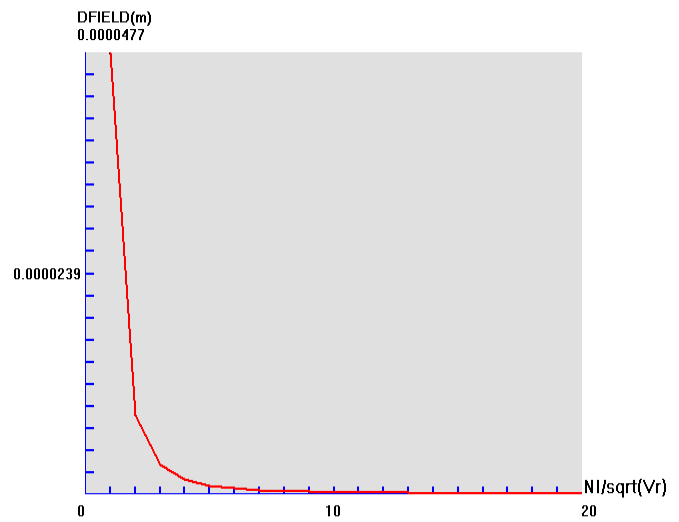


Figure 21- The depth of field (D_{fld}) as a function of excitation parameter ($NI/\sqrt{V_r}$) at ZMC for magnetic lens with using the exponential field model.

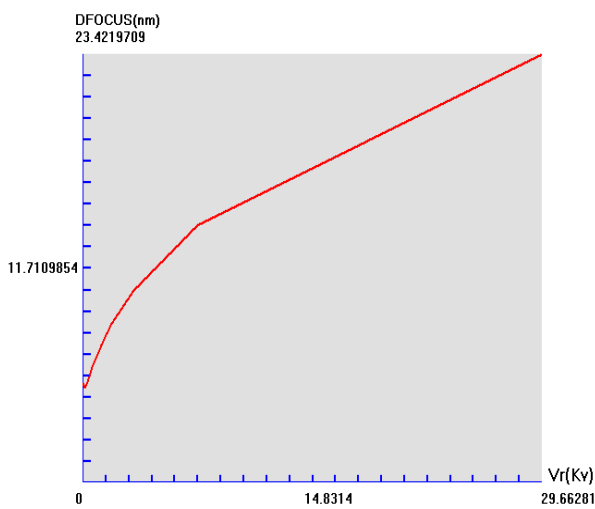


Figure 22- The depth of focus (D_{foc}) as a function of accelerating voltage (V_r) at ZMC for magnetic lens with using the exponential field model.

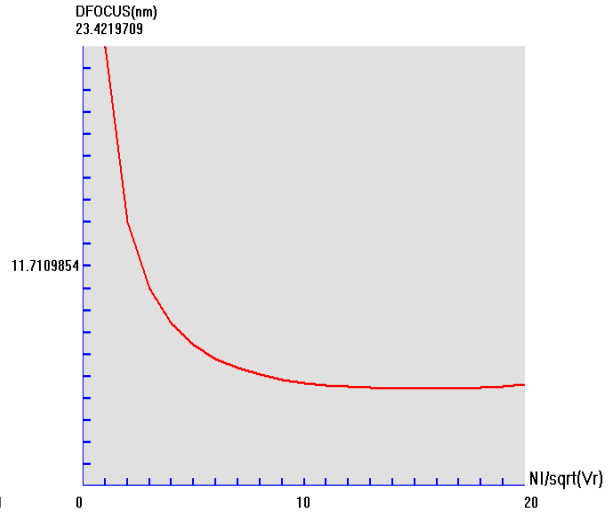


Figure 23- The depth of focus (D_{foc}) as a function of excitation parameter ($NI/\sqrt{V_r}$) at ZMC for magnetic lens with using the exponential field model.

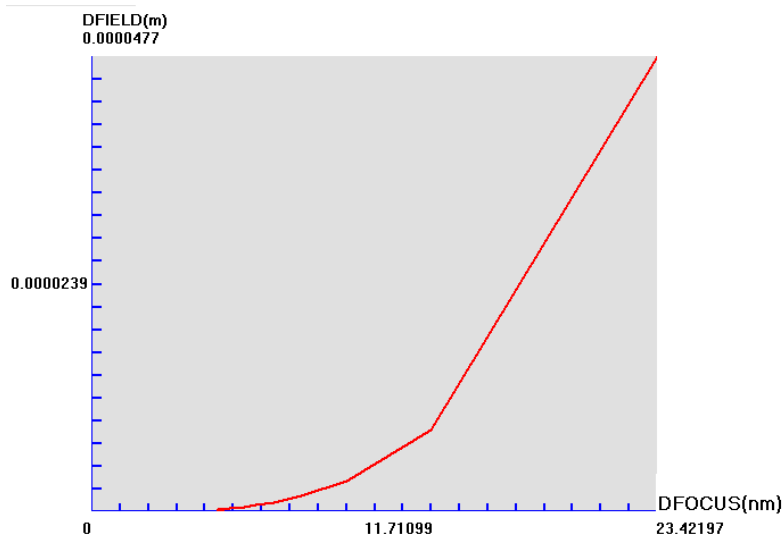


Figure 24- The depth of field (D_{fld}) as a function of depth of focus (D_{foc}) at ZMC for magnetic lens with using the exponential field model.

References

- [1] Hasan, H. S. “Building a New Software of Electromagnetic Lenses (CADTEL)”. SciPress Ltd., Switzerland, *International Letters of Chemistry, Physics and Astronomy*, vol. 9, pp. 46-55, 2013.
- [2] Nagasao, K.; Takebe, M.; Ushio, W.; Fujita, S.; Ohye, T.; Shimoyama, H. “Upgraded G-optk program for electron gun characterization”. *Nuclear Instruments and Methods in Physics Research Section A: Accelerators, Spectrometers, Detectors and Associated Equipment*, vol. 645, Issue 1, pp. 321-326, 2011.
- [3] Al-Shamma M. T., and Al-Khashab M. A. “Improvement of the Optical Performance of the Geometrical Parameters of Snorkel Magnetic Lens”. *Raf. J. Sci.*, vol. 28, no.1, pp.85-97, 2019.

- [4] Hawkes P. W. and Hýtch M.. *Advances in Imaging and Electron Physics Including Proceedings CPO-10. copyright Elsevier Inc., 1st edition*, vol. 212, pp.27-34, 2019.
- [5] Al-Obaidi H. N., Al-Azawy A. A. R. “An Investigation Tool for Analyzing Electrostatic Lenses”. *journal of college of education*, vol.1, no.1. pp. 39 -64, 2016.
- [6] Yang T., Li J. J., Song Y. F., Fan K. J. Study on spherical aberration correction of solenoid lens in ultrafast electron diffraction. 10th Int. Particle Accelerator Conf., IPAC 2019, Melbourne, Australia, JACoW Publishing, pp. 213-216, 2019.
- [7] Hasan, H.S. A Computer Aided Designing Tools for Electron Lenses A Computer Aided Designing Tools for Electron Lenses. Ph.D. Thesis, the University of Mustansiriyah, Baghdad, Iraq. 2012.
- [8] Kato M., and Tsuno K. “Optimization of Electron Lens Shape Giving Minimum Spherical Aberration Coefficient”. *IEEE Transaction on Magnetic*, vol. 26, pp.1023-1025, 1990.
- [9] Liao, Y. *Practical Electron Microscopy and Database. Second Edition*, 2018.
- [10] Hawkes, P.W. *Advances in imaging and electron physics. Vol.123, Elsevier Science USA, Academic press: London*, 2002.
- [11] Orloff J. *Handbook of Charged Particle Optics. 2nd edition by Taylor and Francis group, CRC PRESS, London*, 2009.
- [12] Egerton R. F. *Physical Principles of Electron Microscopy. Springer, USA*, 2005.
- [13] Williams, D. B.; Carter, C. B. *Transmission Electron Microscopy. A Textbook for Materials Science, Springer*, 2009.